IMPLICATIONS OF DEGENERATE MODE MIXING IN UK XFEL SC CAVITIES

A. J. Gilfellon[1,2*], A. E. Wheelhouse[1], P. H. Williams[1], B. Muratori[1], STFC, UK
R. M. Jones[1], University of Manchester, UK
[1]also at Cockcroft Institute, Daresbury Laboratory, UK
[2]also at University of Manchester, UK

Abstract

The UK XFEL (United Kingdom X-ray Free Electron Laser) is a proposed accelerator facility that will use predominantly superconducting RF structures to accelerate and manipulate the transiting electron bunches. Deviations from design longitudinal length of these Niobium RF cavities, or cells within, caused by errors in manufacturing, fabrication tolerances, assembly and installation can lead to modes becoming frequency degenerate. This gives rise to mode mixing, whereby the component modes combine to form additive and subtractive field distributions. Here we look at the mixing of transverse magnetic (TM) modes and locate problematic combinations where field strength enhancements can lead to increased on-axis loss factors and dipole kick factors, both of which can have adverse effects on the beam emittance and energy.

INTRODUCTION

The frequency of any given mode in an RF cavity is dependent on the longitudinal length of the structure (d), the degree of the dependence being strongly linked to the p index in its mode designation (TM_{mnp} or TE_{mnp}), which codifies the degree of modal structure in the longitudinal dimension. Here, TM and TE signify transverse magnetic and electric fields respectively. If the longitudinal length of the structure (d) is varied sequentially, some modes' frequencies change and undergo frequency migration, in some cases a consequence of this is that the frequency of two modes can become indistinguishable or degenerate.

When this occurs, and concentrating on the electric fields, the two eigenmodes (E_1 and E_2) combine together to form mixed modes, either additively or subtractively: $E_{\pm} = E_1 \pm E_2$. The presence of these fields with their unexpected spatial distributions can have consequences for the beam, in that the mixed fields can have a low presence at cell irises and be hard to couple out and have enhanced field strengths and can deliver unexpected longitudinal or transverse kicks. This phenomenon was recently noted in relation to the PIP-II HB650 cavities [1, 2]. The present study investigates this interaction as it relates to the cavities proposed for the UK XFEL project [3, 4].

* anthony.gilfellon@stfc.ac.uk

OVERVIEW OF MODE MIXING

Sources of Variation in Structure Length, d

For ultra-relativistic electron beams accelerated by π-mode, the design length d_0 of a cavity mid-cell is $\lambda_{010}/2$, where λ_{010} is the wavelength of the accelerating mode.

Deviations from d_0 in relatively malleable niobium SC cavities can occur for a number of reasons; manufacturing errors, deformation during transport or installation, they can also occur intentionally from the need to tune cells to attain field-flatness and the cavity as a whole to deliver the operating frequency. Known differences in d are introduced by fabrication, assembly field-flatness tuning and frequency tuning are known to be small ($< 1\%$) [5, 6].

Types of Field Interactions to Be Considered

The scope of this study is restricted to investigating only TM-TM mixing since, due to the z-direction of the beam's velocity vector, only E_z will affect the beam longitudinally or transversely (via Panofsky-Wenzel [7]). Within the limit of a fully relativistic beam the transverse kicks delivered by transverse electric and magnetic fields are equal in magnitude and opposite in direction, so cancel each other out. TE like modes will contribute little to the z-component of the electric field and so are omitted from this investigation.

TM modes can be categorised into groups by their azimuthal mode index m defining monopole, dipole, quadrupole modes with $m = 0$, $m = 1$ and $m = 2$ respectively. Here we initially consider both homotypic mixing (monopole-monopole, dipole-dipole and quadrupole-quadrupole) and the broader group of heterotypic mixing (monopole-dipole, dipole-quadrupole or monopole-quadrupole) to show the TM-TM population is distributed in the $\ell - \hat{f}$ plane (see Eqs. (1) and (2)). When analysing the resultant mixed fields and their loss or kick factors, only homotypic TM interactions are included since the mixed fields remain essentially monopolar, dipolar, or quadrupolar. Heterotypic mixed fields require deeper consideration and are deferred to future work.

CST-BASED E.M. CAVITY SIMULATIONS

This study examines the three cavity types present in the UK XFEL machine; TESLA, $c650$ and 3HC. Some relevant characteristics of these cavities are outlined in Table 1. The $c650$ cavity is based on the PIP-II HB650 [1] and adapted to be consistent for use with ultra-relativistic electrons, whereby the mid-cell longitudinal cell lengths were

Table 1: Cavity Specifications for the UK XFEL Machine

Name	$\omega/2\pi$ [MHz]	Number of Cells	d_0 [mm]
TESLA	1300	9	115.3
$c650^*$	650	5	230.6
3HC**	3900	9	38.4

*Adapted from the PIP-II HB650 cavity [1].

**EuXFEL [8] and SHINE [9] variants.

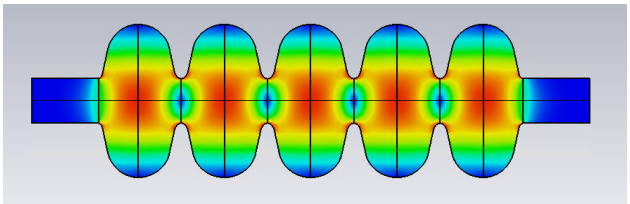

Figure 1: The $c650$ cavity adapted from the PIP-II HB650 [1] showing the accelerating π-mode E-field rendered in CST.

extended to be $\lambda_{010}/2 = 230.6\,\text{mm}$ with the equator radii adjusted to regain the target cavity frequency of 650 MHz and the beampipe radii altered to attain field flatness > 99%. This prototype RF design has not been optimised beyond the stated parameters. See Fig. 1 for the geometry and TM_{010} π-mode rendered in CST [10] .

In each case the mid-cell of each cavity is modelled in CST and d is varied in a parameter sweep from 90% to 110% of d_0. The CST macro that creates the elliptical cavity for the TESLA and 3HC model geometries failed at $\ell < 0.93$ and $\ell < 0.95$ respectively, as discontinuities appeared at the boundaries, hence the constrained ℓ spans for those studies.

RESULTS

To best display the parameter sweep results, and for ease of comparison between cavities, we adopt the same convention as [2], where by we define $\hat{f}$ by normalising the HOM frequencies to that of the main accelerating mode

$$\hat{f} = \frac{f_{mnp}}{f_{010}}, \tag{1}$$

where f_{mnp} is the frequency of the HOM. We also normalise the longitudinal length to the design length and define a length factor (ℓ) such that

$$\ell = \frac{d}{d_0} = \frac{2d}{\lambda_{010}} = \frac{2df_{010}}{c}. \tag{2}$$

Power law fits were extrapolated past the CST simulation range in order to pin-point potential additional degenerate mode mixing (although CST numerical simulations will be required to confirm these results). The results for the TESLA, $c650$ and 3HC mid-cell CST parameter sweeps are displayed in Figs. 2, 3 and 4 respectively, with homotypic mode crossings highlighted by red circles.

Where homotypic combinations involved parent modes of $m = 1$ (dipoles pairs), the kick factors were obtained by

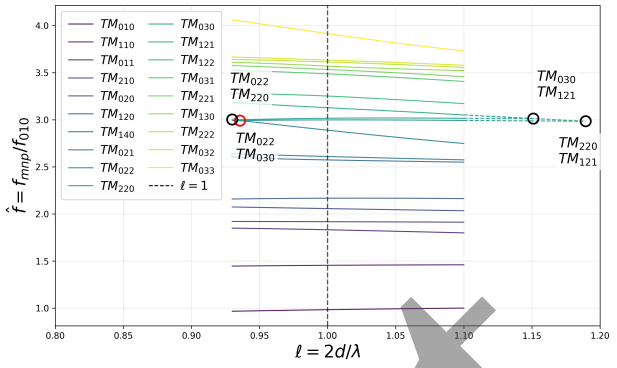

Figure 2: Results of the FM parameter sweep for the TESLA mid-cell. Mode crossings are indicated by circular markers with homotypic intersections highlighted in red. Data extrapolated by power-law fits are depicted by dashed lines.

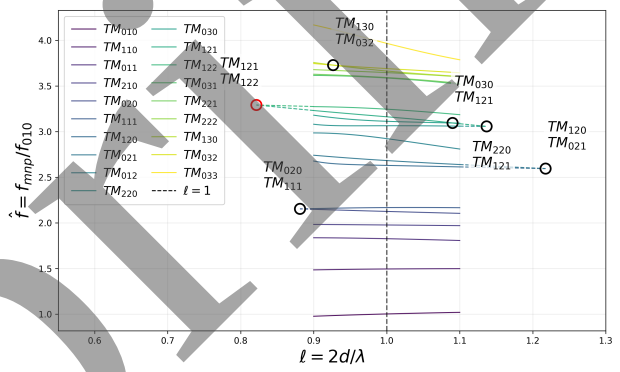

Figure 3: Results of the FM parameter sweep for the $c650$ mid-cell. See caption for Fig. 2 for explanation.

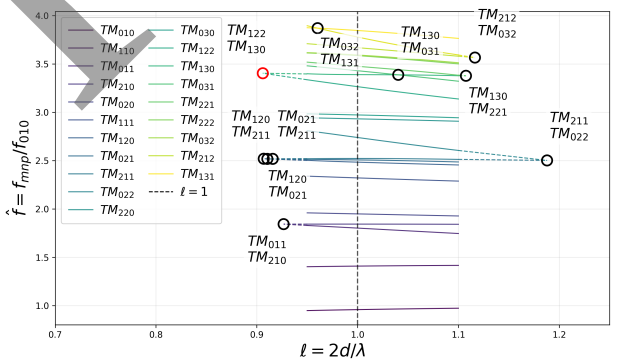

Figure 4: Results of the FM parameter sweep for the 3HC mid-cell. See caption for Fig. 2 for explanation. Shown here are the SHINE 3HC [9] results, although there was no appreciable difference between the EuXFEL and SHINE variants.

integrating E_z along radially offset trajectories, from which the loss factors was calculated, and subsequently the kick factor, see [11] for a more detailed treatment. To emphasise the difference in kick factors between the native parent modes and the mixed modes, we define a ratio $R_{\perp\max}$ which is the ratio of the greater kick factor of the two mixed fields

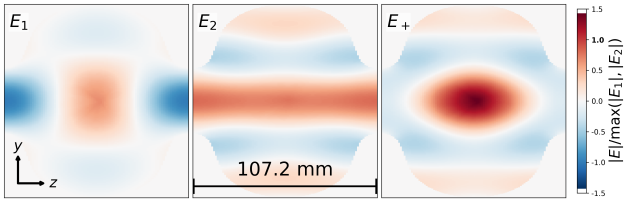

Figure 5: The homotypic monopole mixing in the TESLA mid-cell showing the E_z fields of parent TM_{022} and TM_{030} modes (E_1 & E_2) and the mixed E_+ mode, where $E_+ = E_1 + E_2$. The colour scale is normalised to $\max(E_1, E_2)$ to better demonstrate the E_z field strength enhancement of the mixed mode. In this case there is an increase in $\max(E_z)$ of 77% compared to $\max(E_1, E_2)$.

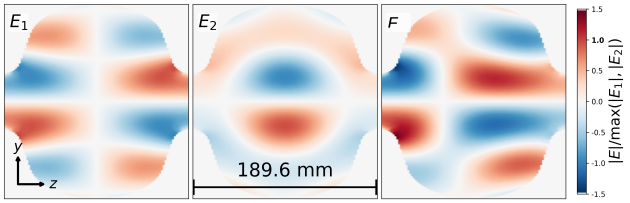

Figure 6: The homotypic monopole mixing in the $c650$ mid-cell showing the E_z fields of parent TM_{121} and TM_{122} modes (E_1 & E_2) and the mixed E_+ mode, where $E_- = E_1 - E_2$. See caption for Fig. 5 for explanation. The field strength enhancement here is 55%.

to the greater kick factor of the native fields

$$R_{\perp\max} = \frac{\max\left(k_{\perp+}, k_{\perp-}\right)}{\max\left(k_{\perp E_1}, k_{\perp E_2}\right)}, \tag{3}$$

and to indicate the impact we give the larger of the two kicks of the mixed modes ($k_{\perp\pm,\max}$) generated from the mixed fields

$$k_{\perp\pm,\max} = \max\left(k_{\perp+}, k_{\perp-}\right). \tag{4}$$

Homotypic combinations involving parent modes of $m = 0$ (monopole pairs) can result in either E_+ or E_- having enhanced on-axis loss factors, so an equivalent $R_{\parallel\max}$ and $k_{\parallel\pm,\max}$ are applied to the loss factors according to Eqs. (3) and (4).

The mixed E_z fields for all homotypic combinations resulting in field enhancements are shown for the TESLA TM_{022} TM_{030} in Fig. 5, the $c650$ TM_{121} TM_{122} in Fig. 6 and the 3HC TM_{122} TM_{130} in Fig. 7. In each case the fields are normalised to $\max(|E_1|, |E_2|)$ so that any field enhancement present in the mixed field is evident with values >1. The on-axis loss factor $k_{\parallel\pm,\max}$ and enhancement ratio $R_{\parallel\max}$ are displayed in Table 2.

The TESLA TM_{022} TM_{030} mode combination is of the type highlighted by [2] and we note that the $|E|$ field at the irises of the E_+ mixed mode are diminished by 24% and 30% w.r.t. E_1 and E_2 respectively, see Fig. 8.

The kick factor $k_{\perp\pm,\max}$ and enhancement ratio $R_{\perp\max}$ for the two dipole pair combinations present in both the $c650$ and 3HC are displayed in Table 2.

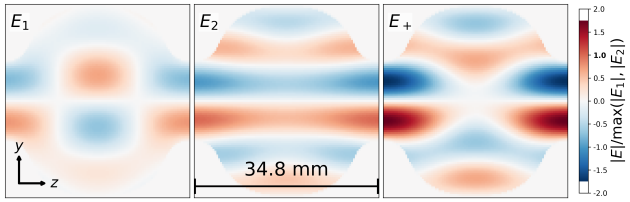

Figure 7: The homotypic monopole mixing in the 3HC mid-cell showing the E_z fields of parent TM_{121} and TM_{122} modes (E_1 & E_2) and the mixed E_+ mode, where $E_+ = E_1 + E_2$. See caption for Fig. 5 for explanation. The field strength enhancement here is 75%.

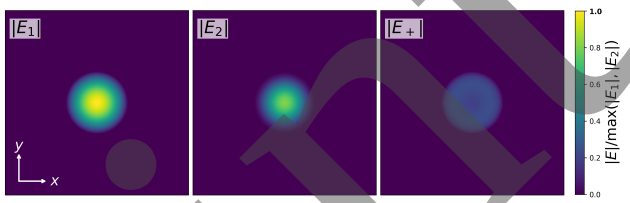

Figure 8: Plots demonstrating the diminished $|E|$ at the irises of E_+ compared to both E_1 (24%) and E_2 (30%) for the homotypic monopole interaction in the TESLA mid-cell.

Table 2: On-axis Loss ($m = 0$) and Kick Factor ($m = 1$) Data for Homotypic Mode Crossings

Cavity	E_1 TM	E_2 TM	ℓ	$\hat{f}$	$k_\parallel$ [V/pC/m]	$k_\perp$ [V/pC/m^2]	$R_{\max}$
TESLA	022	030	0.93	3.00	1.072	–	2.03
$c650$	121	122	0.82	3.29	–	0.0031	1.12
3HC	122	130	0.91	3.40	–	5.64	3.10

FINAL REMARKS

The suite of simulations undertaken in this work have demonstrated mixing of degenerate electromagic modes can result in significant enhancement in the equivalent kick factors. In fact, in the worst-case scenario the kick factors are larger by a factor of three or more from their fundmental, or native, eigenmodes. We haven't explored the effect of these degenerate modes on the beam dynamics. Moreover, future work is anticipated to be focussed on beam dynamics simulations with the codes, PLACET [12] and RF-Track [13], with a view to ascertaining the impact on the beam emittance and on the energy spread for UK-XFEL

ACKNOWLEDGEMENTS

The authors acknowledge the help and input from Andrei Lunin, Detlef Reschke, Alexey Sulimov, Jens Iversen, Nirav Joshi, David Walsh and Aaron Farricker.

REFERENCES

[1] M. Ball *et al.*, "The PIP-II conceptual design report," Fermilab, Batavia, IL, USA, Rep. FERMILAB-DESIGN-2017-01, FERMILAB-TM-2649-AD-APC, 2017.

[2] V. Yakovlev, A. Lunin, and S. Belomestnykh, "Interaction of degenerate higher order modes in periodic accelerating structures," presented at HOMSC2025, DESY, Hamburg, Germany, Oct. 6–8, 2025.

[3] UK XFEL Collaboration, "UK X-ray free electron laser science case," STFC, UK, Rep. STKA00183.07, v3, 2023.

[4] D. J. Dunning *et al.*, "UK XFEL: the UK vision for next-generation XFELs," presented at IPAC'26, Deauville, France, May 2026, paper THV2003, this conference.

[5] J. Corno *et al.*, "Uncertainty modeling and analysis of the European X-ray free electron laser cavities manufacturing process," *Nucl. Instrum. Methods Phys. Res. A*, vol. 971, p. 164135, 2020. doi:10.1016/j.nima.2020.164135

[6] A. A. Sulimov, "RF measurements for quality assurance during SC cavity mass production," in *Proc. SRF'15*, Whistler, BC, Canada, Sep. 2015, paper WEBA02, pp. 955–960. doi:10.18429/JACoW-SRF2015-WEBA02

[7] W. K. H. Panofsky and W. A. Wenzel, "Some considerations concerning the transverse deflection of charged particles in radio-frequency fields," *Rev. Sci. Instrum.*, vol. 27, p. 967, 1956. doi:10.1063/1.1715427

[8] P. Zhang, N. Baboi, and R. M. Jones, "Eigenmode simulations of third harmonic superconducting accelerating cavities for FLASH and the European XFEL," DESY, Hamburg, Germany, Rep. DESY 12-101, 2012.

[9] Y. X. Zhang, J. F. Chen, and D. Wang, "RF design optimization for the SHINE 3.9 GHz cavity," *Nucl. Sci. Tech.*, vol. 31, p. 73, 2020. doi:10.1007/s41365-020-00772-z

[10] Dassault Systèmes, "CST Studio Suite," SIMULIA, Dassault Systèmes, Vélizy-Villacoublay, France.

[11] A. J. Gilfellon, A. E. Wheelhouse, B. Muratori, P. Williams, and R. M. Jones, "Dipole mode wakefields and beam dynamics tracking simulations for the UK XFEL main accelerating linacs," presented at IPAC'26, Deauville, France, May 2026, paper THP2085, this conference.

[12] R. Costa, A. Latina, and M. Olvegård, "PLACET3: 6D tracking through PETS and accelerating structures wakefields," *J. Phys. Conf. Ser.*, vol. 2687, p. 062027, 2024. doi:10.1088/1742-6596/2687/6/062027

[13] A. Latina, "RF-Track reference manual," CERN, Geneva, Switzerland, 2024. doi:10.5281/zenodo.3887085